Comparative roles of *pp* chain reactions as a trigger for suprathermal processes in the solar core

Victor T. Voronchev,[1,*] Yasuyuki Nakao,[2,†] and Yukinobu Watanabe[3,‡]
[1]*Skobeltsyn Institute of Nuclear Physics, Lomonosov Moscow State University, Moscow 119991, Russia*
[2]*Green Asia Education Center, Kyushu University, 6-1 Kasuga-koen, Kasuga, Fukuoka 816-8580, Japan*
[3]*Department of Advanced Energy Engineering Science, Kyushu University, 6-1 Kasuga-koen, Kasuga, Fukuoka 816-8580, Japan*
(Received 5 June 2017; revised manuscript received 22 August 2017; published 13 November 2017)

Continuing the study of suprathermal effects in the solar core [Phys. Rev. C **91**, 028801 (2015); J. Phys. G **44**, 045202 (2017)], we examine the roles of different *pp* chain processes generating fast α particles as trigger for suprathermal B(α,p)A reactions neglected in standard solar model simulations. The suprathermal impact on the balance of the $p + {}^{17}\mathrm{O} \rightleftarrows \alpha + {}^{14}\mathrm{N}$ reactions involved in the solar CNO cycle is determined. It is obtained that MeV α particles born in the ${}^{7}\mathrm{Li}(p,\alpha)\alpha$ and ${}^{3}\mathrm{He}({}^{3}\mathrm{He},2p)\alpha$ reactions are the main agents that are able to crucially change the reaction balance through an appreciable enhancement of the reverse (α,p) reaction. The comparative role of the $p + {}^{7}\mathrm{Li}$ and ${}^{3}\mathrm{He} + {}^{3}\mathrm{He}$ α particles is clarified. It is found that the former particles control the reverse ${}^{14}\mathrm{N}(\alpha,p){}^{17}\mathrm{O}$ reaction in the inner core, while the latter ones play a dominant role in the outer core, additionally increasing the (α,p) reaction rate by several times and providing favorable conditions for synthesis of some elements. In particular, we show that the total suprathermal enhancement of ${}^{17}\mathrm{O}$ and ${}^{18}\mathrm{O}$ mass fractions in the outer core can reach $\sim$80 or 50, depending on a model for α-particle energy loss used in the simulation. In this context, we note that the $p + {}^{7}\mathrm{Li}$ α particles alone provide the mass fraction enhancement by a factor of 20 or less.

DOI: 10.1103/PhysRevC.96.055803

I. INTRODUCTION

In high-temperature astrophysical objects, energetic non-Maxwellian particles of various origins are able to enhance the rates of nuclear reactions in the matter. Such particles (both ions and neutrons) are commonly produced in exoergic reactions and also can be created by recoil in close collisions between bulk matter species and energetic reaction products. The phenomenon of reaction enhancement has a universal nature and in a greater or lesser degree can manifest at exploding as well as nonexploding stages of object evolution.

This should be taken into account to accurately simulate chain reaction kinetics in astrophysical plasmas. In the presence of energetic particles, the balance between the rate parameters $\langle\sigma v\rangle$ for forward $i + j \rightarrow k + l$ and reverse $k + l \rightarrow i + j$ reactions can depart from a standard relation for thermal Maxwellian reactants that gives $\langle\sigma v\rangle_{kl\rightarrow ij} \propto \langle\sigma v\rangle_{ij\rightarrow kl} \exp(-Q/T)$ [1]. The quantity Q is the Q value of the exoergic forward reaction and T is the plasma temperature expressed in units of energy. A correction to this standard relation mainly results from an appreciable enhancement of the endoergic reverse reaction caused by suprathermal non-Maxwellian reactants. This was clearly demonstrated on the example of processes occurring in the primordial [2] and solar core [3] plasma. It was recognized that the suprathermal effect is more pronounced in the Sun—in particular, because the comparatively low temperature of the solar core $T \lesssim 1.4$ keV strongly suppresses the thermal parameters $\langle\sigma v\rangle$ for reverse reactions. This finding has served as an impetus for a detailed study of suprathermal processes in the solar interior.

Such a study was carried out in a recent paper [4]. An original model for the description of suprathermal processes in the solar core was applied to examine the behavior of $p + {}^{17}\mathrm{O} \rightleftarrows \alpha + {}^{14}\mathrm{N}$ reactions in the CNO cycle "irradiated" by fast α particles. It was found that 8.674-MeV α particles produced in the ${}^{7}\mathrm{Li}(p,\alpha)\alpha$ reaction of the *pp* chain can crucially change the balance of these processes, increasing the reverse (α,p) reaction rate. This phenomenon was shown to form a nonstandard (α,p) nuclear flow that can modify running of the CNO cycle and, in particular, increase the abundances of ${}^{17}\mathrm{O}$ and ${}^{18}\mathrm{O}$ isotopes in the outer core region.

Although the ${}^{7}\mathrm{Li}(p,\alpha)\alpha$ reaction generates highly energetic products, some other processes of the *pp* chain can also produce fast α particles. The role of these particles has still not been clarified. At the same time, rough estimates for one of such processes—the ${}^{3}\mathrm{He}({}^{3}\mathrm{He},2p)\alpha$ reaction—suggest that the ${}^{3}\mathrm{He} + {}^{3}\mathrm{He}$ α particles can also contribute to the suprathermal ${}^{14}\mathrm{N}(\alpha,p){}^{17}\mathrm{O}$ rate [4].

The main objective of the present paper is to advance the previous studies [3,4] by taking into account the role of fast α particles produced in different *pp* chain processes. The total picture of suprathermal impact on the $p + {}^{17}\mathrm{O} \rightleftarrows \alpha + {}^{14}\mathrm{N}$ reactions will be composed and its influence on the solar CNO cycle will be determined.

II. FAST α PARTICLE PRODUCTION IN INDIVIDUAL *pp* CHAIN PROCESSES

Two types of *pp* chain processes can produce fast α particles. These are (i) exoergic nuclear reactions and (ii) decays of unstable nuclides. The following description of particle emission is used for these cases:

*voronchev@srd.sinp.msu.ru
†nakao@nucl.kyushu-u.ac.jp
‡watanabe@aees.kyushu-u.ac.jp

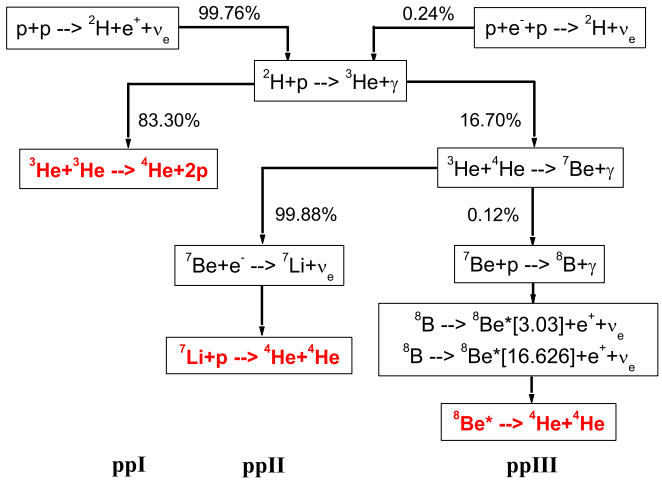

FIG. 1. The three principal branches of the solar pp chain.

(i) The emission rate $R_{\alpha,ij}$ of α particles in a $i+j$ reaction is given by

$$R_{\alpha,ij} = N_\alpha R_{ij}, \tag{1}$$

where N_α is the number of α particles produced per pair of (ij) and R_{ij} is the $i+j$ reaction rate

$$R_{ij} = (1+\delta_{ij})^{-1} n_i n_j \langle \sigma v \rangle_{ij}. \tag{2}$$

In Eq. (2), n_i and n_j are the number densities of particles i and j, respectively, and $\langle \sigma v \rangle_{ij}$ is the $i+j$ reaction rate parameter (briefly, the $i+j$ reactivity). For the Maxwellian reactants the $i+j$ reactivity has a well-known form

$$\langle \sigma v \rangle_{ij} = \left(\frac{8}{\pi \mu_{ij}}\right)^{1/2} \frac{1}{T^{3/2}} \int_0^\infty E \sigma_{ij}(E) \exp\left(-\frac{E}{T}\right) dE, \tag{3}$$

where μ_{ij} is the reduced mass of particles i and j, E is their total kinetic energy in the center-of-mass frame, T is the plasma temperature in units of energy, and σ_{ij} is the $i+j$ reaction cross section in the matter. The effect of electron screening in the solar core plasma is taken into account within a weak-screening approximation [5] satisfactorily describing this phenomenon for particles with charge numbers $Z_i Z_j \lesssim 10$ [6]. According to this approach, the cross section σ_{ij} in the plasma and the cross section $\sigma_{ij,b}$ for bare nuclei are related as

$$\sigma_{ij} = \exp\left(\frac{Z_i Z_j e^2}{T \lambda'_D}\right) \sigma_{ij,b}, \tag{4}$$

where λ'_D is the Debye shielding length corrected for electron degeneracy in the core.

(ii) The emission rate $R_{\alpha,b}$ of α particles in the decay of unstable nuclides b is

$$R_{\alpha,b} = N'_\alpha \frac{n_b}{\tau}, \tag{5}$$

where N'_α is the number of α particles released per decay, n_b is the number density of nuclides b, and τ is their mean lifetime.

Figure 1 schematically presents the solar pp chain. Shown are the three principal branches ppI, ppII, and ppIII. Each of them involves processes generating α particles that are listed in Table I. It follows from Eqs. (1) and (5) that the α particle emission rates are

$$R_{\alpha,^3\mathrm{He}^3\mathrm{He}} = \tfrac{1}{2} n_{^3He} n_{^3He} \langle \sigma v \rangle_{^3\mathrm{He}^3\mathrm{He}\to\alpha 2p}, \tag{6}$$

$$R_{\alpha,\mathrm{p}^7\mathrm{Li}} = 2\, n_p n_{^7Li} \langle \sigma v \rangle_{p^7\mathrm{Li}\to 2\alpha}, \tag{7}$$

$$R_{\alpha,^8\mathrm{Be}^*[16.626]} = 2\frac{n_{^8B}}{\tau}\eta_1, \tag{8}$$

$$R_{\alpha,^8\mathrm{Be}^*[3.03]} = 2\frac{n_{^8B}}{\tau}\eta_2, \tag{9}$$

where $\tau = 1.109$ s in the mean lifetime of ^{8}B, $\eta_1 \simeq 0.12$ and $\eta_2 \simeq 0.88$ are the branching ratios for the β^+ decay of ^{8}B into two excited states of ^{8}Be* with excitation energies E_x of 16.626 MeV and 3.03 MeV, respectively, [7].

Figure 2 shows the calculated α-particle emission rates in the solar core. The radial profiles of temperature and element number densities for the present-day Sun predicted by MESA [8] were used in the calculation.[1] The ^{3}He(^{3}He,2p)α and ^{7}Li(p,α)α reactivities for bare nuclei $\langle \sigma v \rangle_b$ were taken from the NACRE II compilation [9].

It is seen that the ^{3}He(^{3}He,2p)α and ^{7}Li(p,α)α reactions predominantly contribute to the generation of MeV

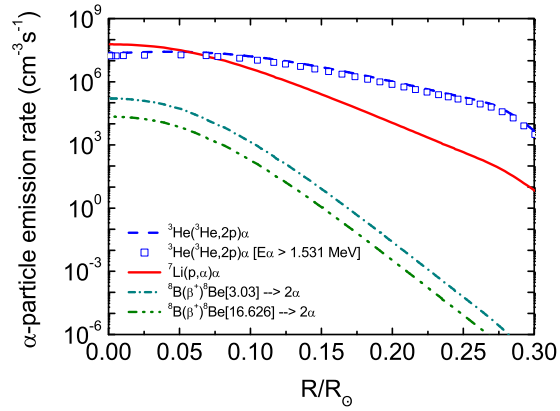

FIG. 2. The emission rates of fast α particles in the pp chain processes. An explanation for the ^{3}He + ^{3}He rate denoted by open squares is given in Sec. III.

TABLE I. Nuclear processes of the pp chain generating fast α particles.

Branch	Reaction	Q (MeV)	$E_{\alpha,0}$ (MeV)
I	^{3}He(^{3}He,2p)α	12.860	0–4.3
II	^{7}Li(p,α)α	17.348	8.674
III	^{8}B(β^+)^{8}Be*[16.626] $\to 2\alpha$	18.072	8.359[a]
III	^{8}B(β^+)^{8}Be*[3.03] $\to 2\alpha$	18.072	1.561[a]

[a]The value of $E_{\alpha,0}$ may change within the half-width of the ^{8}Be excited state being considered.

[1]For some values of T and n_i adopted by us, see Ref. [4].

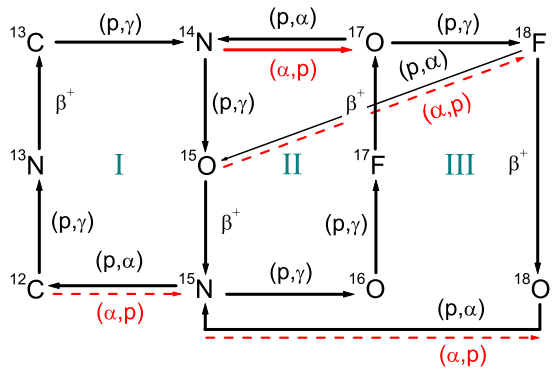

FIG. 3. The solar CNO cycle. Shown are the three branches I, II, and III.

α particles. At the same time, the fluxes of α particles from both $^8\mathrm{B}(\beta^+)^8\mathrm{Be}^* \to 2\alpha$ processes prove to be rather low, suggesting that they are unlikely to be able to provide appreciable suprathermal effects in the solar core. However, to make a final conclusion on this matter, one needs to calculate and compare the main characteristics of suprathermal reactions induced by all these α particles. It will be done in Sec. III.

III. SUPRATHERMAL IMPACT ON THE CNO CYCLE

Standard solar models rely on the thermal nuclear reaction network, so reverse B(α,p)A reactions play a negligible role here as their reactivities $\langle\sigma v\rangle$ are dramatically suppressed by a factor $\exp(Q/T)$. At the same time, in the scenario we develop fast α particles from the *pp* chain processes can "irradiate" the CNO cycle in a natural way and appreciably enhance some (α,p) processes involved in it.

The CNO cycle is schematically presented in Fig. 3. Both forward and reverse two-body reactions $p + \mathrm{A} \rightleftarrows \alpha + \mathrm{B}$ are shown. To describe these competing processes properly, one needs to know their rate parameters $\langle\sigma v\rangle$ with good accuracy. Such data for the forward (p,α) reactions are fairly well represented in the literature. We can refer the reader to review papers on solar fusion cross sections [10,11] as well as various compilations—beginning from pioneering nuclear databases for astrophysics [12–14] and up to more recent works in the field, e.g., Refs. [9,15,16]. At the same time, reliable nuclear data on the endoergic reverse (α,p) reactions still remain rather scanty. To calculate suprathermal B(α,p)A rates, one needs to know the total (α,p) cross sections for α-particle energies from $\sim$9 MeV (see Table I) down to the reaction thresholds. In Fig. 3, the dashed arrows denote reverse (α,p) reactions which have been poorly studied at such energies. Available information on these processes—both experimental measurements and theoretical estimates—is still insufficient to obtain the reliable total cross sections and calculate the suprathermal rates. The only (α,p) reaction in Fig. 3 for which the total cross section can be inferred from existing data [17] is $^{14}\mathrm{N}(\alpha,p)^{17}\mathrm{O}$.

Given all this, we will focus on a pair of the following reactions

$$p + {}^{17}\mathrm{O} \to \alpha + {}^{14}\mathrm{N} \quad (Q = 1.191\ \mathrm{MeV}), \tag{10}$$

$$\alpha + {}^{14}\mathrm{N} \to p + {}^{17}\mathrm{O} \quad (E_{\alpha,\mathrm{thr}} = 1.531\ \mathrm{MeV}), \tag{11}$$

where $E_{\alpha,\mathrm{thr}}$ is the α-particle threshold energy for the reverse (α,p) process. These reactions are responsible for closing (or unclosing) the branch II of the CNO cycle. To compose the total picture of suprathermal impact on the reaction balance, fast α particles of different origins listed in Table I will be taken into account.

The rate $R_{\alpha^{14}\mathrm{N},\mathrm{sprth}}$ of the suprathermal $\alpha + {}^{14}\mathrm{N}$ reaction is the principle quantity for our study. Depending on an α-particle source, this rate is defined as follows:

(a) Monoenergetic and quasimonoenergetic α particles generated in the $^7\mathrm{Li}(p,\alpha)\alpha$ and $^8\mathrm{B}(\beta^+)^8\mathrm{Be}^*[16.626] \to 2\alpha$ processes.[2] In this case, the rate $R_{\alpha^{14}\mathrm{N},\mathrm{sprth}}$ is determined as the product of the α-particle emission rate R_α and the probability $W_{\alpha^{14}\mathrm{N}}$ for an α particle to undergo the $\alpha + {}^{14}\mathrm{N}$ reaction while slowing in the plasma from the birth energy $E_{\alpha,0}$ down to the reaction threshold $E_{\alpha,\mathrm{thr}}$,

$$R_{\alpha^{14}\mathrm{N},\mathrm{sprth}} = R_\alpha \times W_{\alpha^{14}\mathrm{N}}(E_{\alpha,0} \to E_{\alpha,\mathrm{thr}}), \tag{12}$$

where $R_\alpha = R_{\alpha,\mathrm{p}^7\mathrm{Li}}$ and $R_{\alpha,^8\mathrm{Be}^*[16.626]}$ determined by Eqs. (7) and (8). The value of $W_{\alpha,^{14}\mathrm{N}}$ can be calculated within a formalism of in-flight reaction probability,

$$W_{\alpha^{14}\mathrm{N}}(E_{\alpha,0} \to E_{\alpha,\mathrm{thr}}) = 1 - \exp\left[\int_{E_{\alpha,\mathrm{thr}}}^{E_{\alpha,0}} \left(\frac{2E_\alpha}{m_\alpha}\right)^{1/2} \times \frac{n_{^{14}N}\sigma_{\alpha^{14}\mathrm{N}}(E_\alpha)}{(dE_\alpha/dt)}\, dE_\alpha\right], \tag{13}$$

where E_α and m_α are the α-particle energy in the laboratory frame and its mass, respectively, $\sigma_{\alpha^{14}\mathrm{N}}$ is the $\alpha + {}^{14}\mathrm{N}$ reaction cross section, $n_{^{14}N}$ is the $^{14}\mathrm{N}$ number density, and (dE_α/dt) is the rate of α particle energy loss in the matter.

(b) α particles with a continuous source energy spectrum $S(E'_\alpha)$ produced in the $^3\mathrm{He}(^3\mathrm{He},2p)\alpha$ reaction. Taking into account that the spectrum covers the energy range of 0–4.3 MeV, Eq. (12) should be generalized as follows:

$$R_{\alpha^{14}\mathrm{N},\mathrm{sprth}} = R_{\alpha,^3\mathrm{He}^3\mathrm{He}} \times \eta \times \langle W_{\alpha^{14}\mathrm{N}}\rangle, \tag{14}$$

where $R_{\alpha,^3\mathrm{He}^3\mathrm{He}}$ is the α-particle emission rate given by Eq. (6) and η is the fraction of α particles capable of inducing the $\alpha + {}^{14}\mathrm{N}$ reaction

$$\eta = \frac{\int_{E_{\alpha,\mathrm{thr}}}^{E_{\alpha,\max}} S(E'_\alpha)\, dE'_\alpha}{\int_0^{E_{\alpha,\max}} S(E'_\alpha)\, dE'_\alpha}. \tag{15}$$

The energy $E_{\alpha,\max}$ is the maximum $^3\mathrm{He} + {}^3\mathrm{He}$ α particle energy of 4.3 MeV. The quantity $\langle W_{\alpha^{14}\mathrm{N}}\rangle$ in Eq. (14) is the in-flight $\alpha + {}^{14}\mathrm{N}$ reaction probability folded over the source

[2]Since the width Γ_{cm} of the $^8\mathrm{Be}^*[16.626]$ excited state is only 108 keV [7], one can consider α particles produced in the $^8\mathrm{Be}^*$ decay quasimonoenergetic.

energy spectrum $S(E'_\alpha)$,

$$\langle W_{\alpha^{14}\mathrm{N}}\rangle = \frac{\int_{E_{\alpha,\mathrm{thr}}}^{E_{\alpha,\max}} W_{\alpha^{14}\mathrm{N}}(E'_\alpha \to E_{\alpha,\mathrm{thr}}) S(E'_\alpha)\, dE'_\alpha}{\int_{E_{\alpha,\mathrm{thr}}}^{E_{\alpha,\max}} S(E'_\alpha)\, dE'_\alpha}. \quad (16)$$

Finally, Eq. (14) can be rewritten as

$$R_{\alpha^{14}\mathrm{N},\mathrm{sprth}} = R_{\alpha,^3\mathrm{He}^3\mathrm{He}} \frac{\int_{E_{\alpha,\mathrm{thr}}}^{E_{\alpha,\max}} W_{\alpha^{14}\mathrm{N}}(E'_\alpha \to E_{\alpha,\mathrm{thr}}) S(E'_\alpha)\, dE'_\alpha}{\int_0^{E_{\alpha,\max}} S(E'_\alpha)\, dE'_\alpha}. \quad (17)$$

The rate of α-particle energy loss (dE_α/dt) entering Eqs. (13) and (16) plays an important role in the evaluation of the in-flight $\alpha + {}^{14}\mathrm{N}$ reaction probability. Fast α particles lose their kinetic energy through Coulomb elastic scattering (Coul) off background electrons and ions, and also through nuclear elastic scattering (NES) off ambient nuclei. The latter mechanism is commonly subdominant and the majority of particle energy loss comes from the Coulomb collisions.

Several models to treat $(dE_\alpha/dt)_{\mathrm{Coul}}$ in the solar core plasma were tested by us and compared with each other in Ref. [4]. These are as follows:

(1) a standard binary-collision model with a Debye cutoff [18];
(2) a model [19] based on the Fokker-Planck collision theory;
(3) a reduced model [20] which conveniently interpolates between limiting cases for ion energy loss based on classical and quantum kinetic equations;
(4) a model [21] considering that a charged particle passing through a plasma induces an electric field which acts back on this particle and decreases its kinetic energy.

The comparison revealed that the collision models [18–20] give rather close values of $(dE_\alpha/dt)_{\mathrm{Coul}}$ in the solar core which differ by 5–15%, depending on the α-particle energy E_α. At the same time, the model [21] based on the different energy loss mechanism predicts a sizable enhancement of $(dE_\alpha/dt)_{\mathrm{Coul}}$ as the energy E_α increases.

In the present study we employ two approaches [19] and [21] which provide the smallest and largest energy loss rates $(dE_\alpha/dt)_{\mathrm{Coul}}$, respectively. The first model [19] (we refer to it as KAM86) can properly describe $(dE_\alpha/dt)_{\mathrm{Coul}}$ in a plasma with partially degenerate electron component typical of the solar core. According to it

$$\left(\frac{dE_\alpha}{dt}\right)_{\mathrm{Coul}} = \left(\frac{dE_\alpha}{dt}\right)_e + \left(\frac{dE_\alpha}{dt}\right)_i, \quad (18)$$

where the energy loss rate $(dE_\alpha/dt)_j$ through α-electron ($j = e$) and α-ion ($j = i$) scattering is given by

$$\left(\frac{dE_\alpha}{dt}\right)_j = -\frac{8\pi^2 (Z_\alpha Z_j)^2 e^4 (2m_\alpha)^{1/2}}{m_j E_\alpha^{1/2}} \ln\Lambda_{\alpha j} \times J_{j,2}\left[1 - \frac{m_j}{3E_\alpha}\frac{(J_{j,4} + J_{j,1} v_\alpha^3)}{J_{j,2}}\right]. \quad (19)$$

In Eq. (19), the quantity $\ln\Lambda_{\alpha j}$ is the Coulomb logarithm corrected for electron degeneracy using an *ad hoc* procedure [22,23] and

$$J_{j,1}(v_\alpha) = \int_{v_\alpha}^{\infty} v_j f_j(v_j)\, dv_j, \quad (20)$$

$$J_{j,m}(v_\alpha) = \int_0^{v_\alpha} v_j^m f_j(v_j)\, dv_j \quad (m = 2,4), \quad (21)$$

where $f_j(v_j)$ is the velocity distribution function of plasma particles j normalized to their number density n_j. For bulk ions i we assume Maxwellian distributions $f_{i,M}(v_i)$, while for electrons the distribution function $f_{e,\mathrm{FD}}(v_e)$ obeying Fermi-Dirac statistics is used to allow for the effect of electron degeneracy in the solar core.

The second model [21] (we refer to it as SKUP77) provides the rate of α-particle energy loss to plasma electrons of arbitrary degeneracy. Using the random-phase-approximation (RPA) form of quantum-mechanical dielectric function, it was found that

$$\left(\frac{dE_\alpha}{dt}\right)_e = -E_\alpha n_e \frac{Z_\alpha^2 e^4}{T_e^{3/2}} \frac{(2m_e)^{1/2}}{m_\alpha} \frac{4}{3} \times \left[\frac{\pi}{F_{1/2}(\eta)} \frac{1}{e^{-\eta}+1}\right] \ln\Lambda_{\mathrm{RPA}}, \quad (22)$$

where $\eta = \mu/T_e$ is the degeneracy parameter (μ is the chemical potential) and $F_{1/2}(\eta)$ is the standard Fermi integral to order 1/2

$$F_{1/2}(\eta) = \int_0^\infty \frac{x^{1/2}\, dx}{e^{x-\eta}+1}. \quad (23)$$

The quantity $\ln\Lambda_{\mathrm{RPA}}$ is a generalization of the Coulomb logarithm

$$\ln\Lambda_{\mathrm{RPA}} = (1 + e^{-\eta}) \int_0^\infty \frac{k^3}{\left(k^2 + k_0^2\right)^2} \times \left[\exp\left(\frac{\hbar^2 k^2}{8 m_e T_e} - \eta\right) + 1\right]^{-1} dk, \quad (24)$$

where $k_0^2 = k_{\mathrm{D}}^2 F'_{1/2}(\eta)/F_{1/2}(\eta)$ and $k_{\mathrm{D}}^2 = 4\pi n_e e^2/T_e$. This expression for $\ln\Lambda_{\mathrm{RPA}}$ somewhat differs from that originally presented in Ref. [21]. Finally, note once again that Eq. (22) describes only α-e scattering. To obtain the total Coulomb energy loss, one needs to taken into account the contribution of α-i scattering given by Eq. (19) for $j = i$.

The difference between the rates $(dE_\alpha/dt)_{\mathrm{Coul}}$ provided by the SKUP77 and KAM86 models is demonstrated in Fig. 4. Shown is the ratio δ of these two rates. It is seen that δ becomes sizable at high energies, reaching $\sim$1.8 at $E_\alpha = 8.7$ MeV. One needs to note however that Eq. (22) was derived under the assumption that the α-particle velocity v_α is less than the average electron velocity $\langle v_e\rangle$ in the matter. For 8.7-MeV α particles in the solar core, v_α is close to $\langle v_e\rangle$ and therefore some inaccuracy in the SKUP77 prediction can occur.

To calculate the suprathermal $\alpha + {}^{14}\mathrm{N}$ reaction, one needs to know (i) the values of element number densities n_i and temperature T in the solar core, (ii) the reaction cross section $\sigma_{\alpha^{14}\mathrm{N}}$ for the α-particle energy E_α from 8.7 MeV down to the threshold, and (iii) the $^3\mathrm{He} + {}^3\mathrm{He}$ α particle energy spectrum S.

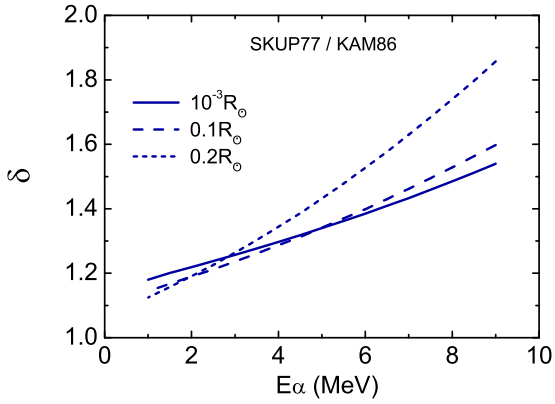

FIG. 4. The ratio δ of the energy loss rate $(dE_\alpha/dt)_{\rm Coul}$ predicted by the SKUP77 model to that obtained for the KAM86 model. Three different regions of the solar core are shown: the inner core ($R = 10^{-3}R_\odot$), the middle core ($R = 0.1R_\odot$), and the outer core ($R = 0.2R_\odot$).

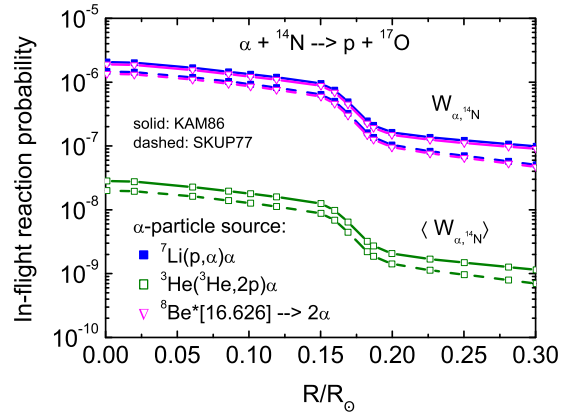

FIG. 5. The probability of the in-flight $^{14}{\rm N}(\alpha,p)^{17}{\rm O}$ reaction in the solar core induced by fast α particles from different pp chain processes. The solid and dashed curves show the results found for the KAM86 and SKUP77 models for the α-particle energy loss, respectively.

In the present work, we adopt the radial profiles $n_i(R)$ and $T(R)$ provided by MESA and employ $\sigma_{\alpha^{14}{\rm N}}(E_\alpha)$ derived from available experimental differential cross section [17] and supplemented with estimates [4] to cover the full energy range of interest.

To specify the $^3{\rm He}+{}^3{\rm He}$ α particle spectrum S entering Eq. (16), some results of a recent paper [24] were used. In this paper, both proton and α particle spectra in the $^3{\rm He}+{}^3{\rm He}\rightarrow 2p+\alpha$ reaction were predicted within an R-matrix model for three-body final states. The prediction was made for a center-off-mass energy $E_1 = 165$ keV. Although the energy of ^{3}He ions in the solar core is thermally distributed, one can focus on energies close to the Gamow peak E_G which determine the majority of the α-particle emission rate $R_{\alpha,{}^3{\rm He}{}^3{\rm He}}$ given by Eq. (6). In the solar core, the value of E_G for the $^3{\rm He}+{}^3{\rm He}$ reaction lies within 15–20 keV, depending on the distance R from the center of the Sun. Both energies E_1 and E_G are thus much less than the reaction Q value and belong to a deep subbarrier region where no resonances occur [25] and the reaction mechanism is unlikely to change. Taking all these into consideration, we assume that the α-particle spectrum does not differ significantly for energies $E_G < E < E_1$ and approximate the shape of $S(E'_\alpha)$ in Eq. (16) by the curve found in Ref. [24]. It starts at zero energy, monotonically goes up as E_α increases, reaches maximum at 3.3 MeV, and then drops, ending at $E_\alpha = 4.3$ MeV. The fraction of α particles η in this spectrum with energies above the $^{14}{\rm N}(\alpha,p)^{17}{\rm O}$ threshold is estimated to be $\sim$0.7. The emission rate of these "active" α particles is shown by open squares in Fig. 2.

Figure 5 presents the probability of the in-flight $^{14}{\rm N}(\alpha,p)^{17}{\rm O}$ reaction in the solar core induced by fast α particles from different processes listed in Table I. Shown are the values of $W_{\alpha^{14}{\rm N}}$ (for the $p+{}^7{\rm Li}$ and $^8{\rm B}(\beta^+)^8{\rm Be}^*[16.626]\,\alpha$ particles) and $\langle W_{\alpha^{14}{\rm N}}\rangle$ (for the $^3{\rm He}+{}^3{\rm He}$ α particles) calculated for the α-particle energy loss rate given by the KAM86 and SKUP77 models. The process $^8{\rm B}(\beta^+)^8{\rm Be}^*[3.03]\rightarrow 2\alpha$ can be excluded from the present consideration. It plays a negligible role because the α-particle birth energy is very close to the $^{14}{\rm N}(\alpha,p)^{17}{\rm O}$ threshold. It is seen from Fig. 5 that the reaction probability $\langle W_{\alpha^{14}{\rm N}}\rangle$ for the $^3{\rm He}+{}^3{\rm He}$ α particles is smaller than $W_{\alpha^{14}{\rm N}}$ by a factor of $\sim$70–80. At the same time, Fig. 2 shows that at $R > 0.07R_\odot$ the emission rate of these particle $R_{\alpha,{}^3{\rm He}{}^3{\rm He}}$ significantly exceeds the other emission rates $R_{\alpha,{\rm p}^7{\rm Li}}$ and $R_{\alpha,{}^8{\rm Be}^*}$, suggesting that the $^3{\rm He}+{}^3{\rm He}$ α particles can contribute to suprathermal processes in the outer core.

This is well demonstrated in Figs. 6 and 7. Here the KAM86 model for $(dE_\alpha/dt)_{\rm Coul}$ is used as an example. Figure 6 shows the total and partial rates $R_{\alpha^{14}{\rm N},{\rm sprth}}$ of the suprathermal $^{14}{\rm N}(\alpha,p)^{17}{\rm O}$ reaction, Eqs. (12) and (14). The comparative role of the partial rates is presented in Fig. 7. It is seen that two sorts of fast α particles contribute to the suprathermal $^{14}{\rm N}(\alpha,p)^{17}{\rm O}$ rate. The $p+{}^7{\rm Li}$ α particles control the reaction

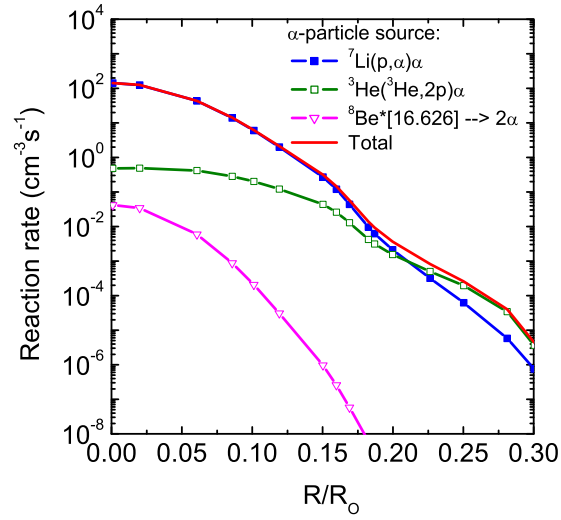

FIG. 6. The solid curve and the curves marked with symbols present the suprathermal $^{14}{\rm N}(\alpha,p)^{17}{\rm O}$ rate in the solar core. Shown are the total as well as partial rates provided by fast α particles from the different pp chain processes. The KAM86 model for the α-particle energy loss rate was used in the calculations.

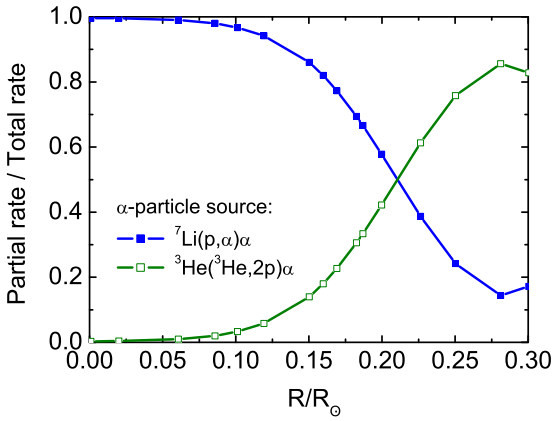

FIG. 7. The contribution of the $p + {}^7\mathrm{Li}$ and ${}^3\mathrm{He} + {}^3\mathrm{He}\,\alpha$ particles to the suprathermal ${}^{14}\mathrm{N}(\alpha,p){}^{17}\mathrm{O}$ rate obtained for the KAM86 model. Shown are the ratios of the partial rates provided by these α particles to the total rate $R_{\alpha^{14}\mathrm{N,sprth}}$.

in the inner core, while the ${}^3\mathrm{He} + {}^3\mathrm{He}$ α particles play a dominant role in the outer core region. The same conclusion was also reached when using the SKUP87 model for the α-particle energy loss. The results for this model differ from those in Fig. 7 by less than ~10% and 3% for the $p + {}^7\mathrm{Li}$ and ${}^3\mathrm{He} + {}^3\mathrm{He}$ α particles, respectively. As for α particles from the ${}^8\mathrm{Be}^*$[16.626] decay, their contribution has proven to be marginal.

It is worthwhile to note that the $p + {}^7\mathrm{Li}$ and ${}^3\mathrm{He} + {}^3\mathrm{He}$ α particles can also control the rates of other suprathermal $\mathrm{B}(\alpha,p)\mathrm{A}$ reactions, unless their thresholds exceed the α-particle energy.

Figure 8 presents a comparison of the forward (p,α) and reverse (α,p) rates for the $p + {}^{17}\mathrm{O} \rightleftarrows \alpha + {}^{14}\mathrm{N}$ reactions. The forward rate has a standard form

$$R_{\mathrm{p}^{17}O} = n_p n_{^{17}O} \langle \sigma v \rangle_{p^{17}\mathrm{O}\to\alpha^{14}\mathrm{N}}, \quad (25)$$

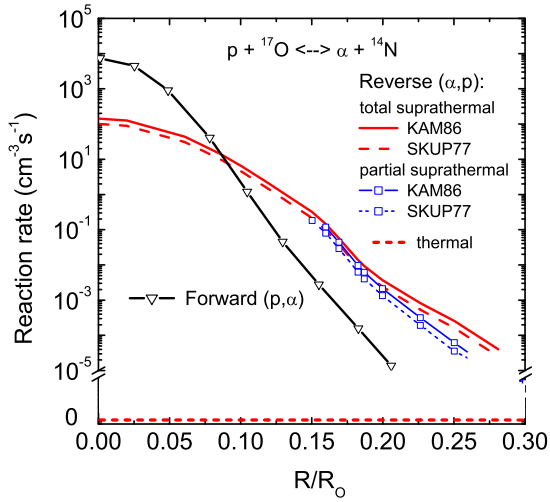

FIG. 8. A comparison of the forward ${}^{17}\mathrm{O}(p,\alpha){}^{14}\mathrm{N}$ and reverse ${}^{14}\mathrm{N}(\alpha,p){}^{17}\mathrm{O}$ reaction rates in the solar core. The partial reverse rate shown here is provided by the $p + {}^7\mathrm{Li}$ α particles.

TABLE II. The solar core temperature T and density ρ provided by MESA for several values of the radius R. The mass fractions and number densities of some elements at the selected radii are given in Ref. [4].

$R/R_\odot$	T (10^6 K)	ρ (g/cm^3)
0.0565	14.775	124.533
0.1011	13.135	87.438
0.1997	9.428	35.479
0.2345	8.382	24.919
0.2502	7.958	21.088
0.2716	7.430	16.732
0.3004	6.797	12.151

where $\langle \sigma v \rangle_{p^{17}\mathrm{O}\to\alpha^{14}\mathrm{N}}$ is the screened thermal reactivity. The respective reactivity for bare reactants was taken from a compilation [15]. The total suprathermal reverse rate $R_{\alpha^{14}\mathrm{N,sprth}}$ for the KAM86 and SKUP77 models is shown together with the partial rate provided by the $p + {}^7\mathrm{Li}$ α particles. For completeness, the thermal reverse rate $R_{\alpha^{14}\mathrm{N,th}}$ is also presented in Fig 8. It can be evaluated using the thermal forward $p + {}^{17}\mathrm{O}$ reactivity as

$$R_{\alpha^{14}\mathrm{N,th}} = c_{\mathrm{rev}} n_\alpha n_{^{14}N} \langle \sigma v \rangle_{p^{17}\mathrm{O}\to\alpha^{14}\mathrm{N}} \exp(-1191/T), \quad (26)$$

where $c_{\mathrm{rev}} = 0.676$ [14] and the plasma temperature T is expressed in keV. One can find that for the solar core conditions $R_{\alpha^{14}\mathrm{N,th}}$ is at most $\sim 10^{-331}$ cm^{-3} s^{-1} and thus is fully negligible.

Figure 8 shows that at $R > 0.2R_\odot$ the total suprathermal ${}^{14}\mathrm{N}(\alpha,p){}^{17}\mathrm{O}$ rate exceeds the partial one by several times. Given in this core region the mass fractions X for some CNO elements are sensitive to the ${}^{14}\mathrm{N}(\alpha,p){}^{17}\mathrm{O}$ reaction [4], the total suprathermal impact of this process on X is of particular interest.

To determine a level of this impact, one needs to incorporate the suprathermal ${}^{14}\mathrm{N}(\alpha,p){}^{17}\mathrm{O}$ reaction induced by the $p + {}^7\mathrm{Li}$ and ${}^3\mathrm{He} + {}^3\mathrm{He}$ α particles in the CNO reaction network. According to Fig. 3, the rate equations for ${}^{14}\mathrm{N}$ and ${}^{17}\mathrm{O}$ number densities should be generalized as follows:

$$\frac{dn_{^{14}N}}{dt} = -n_p n_{^{14}N} \langle \sigma v \rangle_{p^{14}\mathrm{N}\to\gamma^{15}\mathrm{O}} + n_p n_{^{13}C} \langle \sigma v \rangle_{p^{13}\mathrm{C}\to\gamma^{14}\mathrm{N}} + n_p n_{^{17}O} \langle \sigma v \rangle_{p^{17}\mathrm{O}\to\alpha^{14}\mathrm{N}} - R_{\alpha^{14}\mathrm{N,sprth}}, \quad (27)$$

$$\frac{dn_{^{17}O}}{dt} = -n_p n_{^{17}O} \langle \sigma v \rangle_{p^{17}\mathrm{O}\to\alpha^{14}\mathrm{N}} - n_p n_{^{17}O} \langle \sigma v \rangle_{p^{17}\mathrm{O}\to\gamma^{18}\mathrm{F}} + \frac{n_{^{17}F}}{\tau} + R_{\alpha^{14}\mathrm{N,sprth}}, \quad (28)$$

where τ is the mean lifetime of ${}^{17}\mathrm{F}$ and $R_{\alpha^{14}\mathrm{N,sprth}}$ is the total suprathermal ${}^{14}\mathrm{N}(\alpha,p){}^{17}\mathrm{O}$ rate. Thermal reverse reactions in these equations can be ignored.

The respective corrections were incorporated in a stellar nucleosynthesis code [26], and then it was run to evaluate the suprathermal impact on build-up of ${}^{17}\mathrm{O}$ and also ${}^{18}\mathrm{O}$ which follows the former isotope in the CNO diagram. The code was run at constant temperature T and density ρ corresponding to selected values of $R/R_\odot$ (see Table II). The

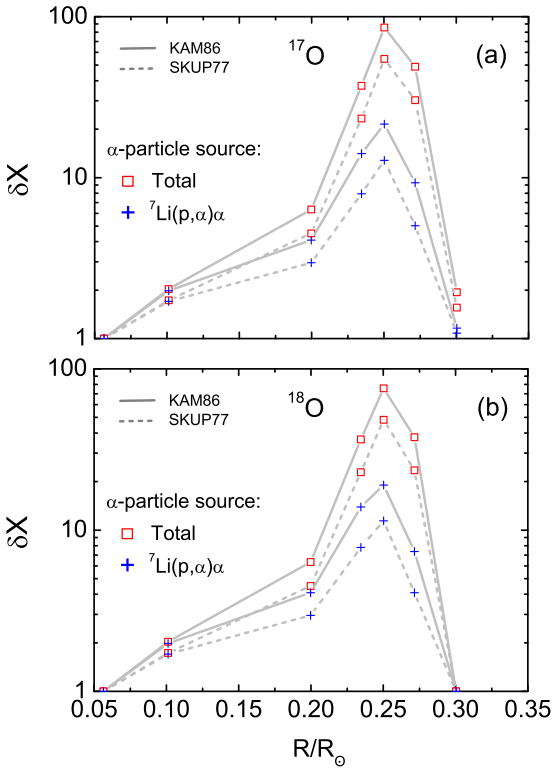

FIG. 9. The mass fraction enhancement $\delta X = X'/X$ for ^{17}O and ^{18}O isotopes caused by the suprathermal ^{14}N$(\alpha,p)^{17}$O reaction. The KAM86 and SKUP77 models for the α-particle energy loss rate were used in the calculations.

results are presented in Fig. 9. Shown is the oxygen mass fraction enhancement $\delta X = X'/X$, where X' (respectively, X) corresponds to the case where the suprathermal ^{14}N$(\alpha,p)^{17}$O reaction is included (respectively, ignored) in the CNO network. Figure 9 demonstrates that the ^{3}He + ^{3}He α particles, controlling the $\alpha + {}^{14}$N rate in the outer core, account for the majority of δX that can reach ~80 (KAM86) or ~50 (SKUP77) at $R = 0.25R_\odot$. The role of the $p + {}^7$Li α particles proves to be less important. The averaged suprathermal effect can be estimated by folding δX over the core volume

$$\langle \delta X \rangle = \frac{3}{r_c^3} \int_0^{r_c} \delta X r^2 \, dr, \tag{29}$$

where $r = R/R_\odot$ and r_c is chosen to be 0.3. It is found that $\langle \delta X \rangle \sim 27$ (KAM86) or 17 (SKUP77), being rather smaller than the peak value of δX.

Finally, it was obtained that the ^{14}N$(\alpha,p)^{17}$O reaction does not alter the ^{14}N abundance, indicating that synthesis of ^{14}N is controlled by processes of the CNO-I cycle.

An interesting issue is how the total action of all suprathermal B(α,p)A reactions shown in Fig. 3 can change the flux of CNO neutrinos through altering the abundances of neutrino-producing nuclides ^{13}N, ^{15}O, and ^{17}F. At present, we are unable to provide quantitative estimates as the (α,p) reactions indicated by the dashed arrows have still been studied poorly and their cross sections should be determined first. Nevertheless, it is possible to make some qualitative predictions. In particular, we expect that additional burn-up of ^{12}C and ^{15}O through the suprathermal ^{12}C$(\alpha,p)^{15}$N and ^{15}O$(\alpha,p)^{18}$F reactions, respectively, can in principle decrease the flux of ^{13}N and ^{15}O neutrinos. As for ^{17}F neutrinos, the situation is difficult to predict now.

In the present work, we restricted consideration to suprathermal reactions induced by α particles, although fast protons can also be present in the solar core—they are generated in the ^{3}He$(^3$He$,2p)\alpha$ reaction. The energy of these protons E_p can reach ~10.5 MeV, so in principle they might open suprathermal channels for (p,α), (p,γ), as well as pp and pep reactions of the CNO cycle and the pp chain. A common feature of these processes, however, is that all of them are exoergic. Therefore, they are not as sensitive to the presence of fast particles in the matter as the endoergic (α,p) reactions that can be activated by MeV α particles only. We have found that the thermalization time of 10.5-MeV protons $\tau_{p,\mathrm{th}}(E_p \to 3T/2)$ in the solar core does not exceed ~2 ps and their effective number density is much less than the number density of bulk protons which ultimately determine the rates of the above reactions. Therefore, the suprathermal impact of the ^{3}He + ^{3}He protons is likely to be negligible.

The last remark concerns a possibility to verify the results for the ^{17}O and ^{18}O abundances using available observational data. One should note some points that make this procedure rather difficult to perform. The results for δX and $\langle \delta X \rangle$ are found for the present-day Sun and not straightforwardly applicable to other stars. The suprathermal effects essentially depend on the stellar core temperature, density, and chemical composition controlling the α particle emission rate, Eq. (1), and the in-flight $\alpha + {}^{14}$N reaction probability, Eqs. (13) and (16). For example, a 10% variation of the keV temperature can change the $p + {}^7$Li and ^{3}He + ^{3}He reactivities $\langle \sigma v \rangle$ by a few times, thus affecting a level of the suprathermal impact. Therefore, the straightforward extrapolation of the present results to stars that entered the red-giant branch and underwent a dredge-up of material to the surface (for some of these stars experimental data on the ^{17}O and ^{18}O abundances are available, e.g., Refs. [27,28]) will suffer from many uncertainties. Finally, Fig. 9 demonstrates the effect of the individual $\alpha + {}^{14}$N reaction. To get the complete picture of the suprathermal impact, the other (α,p) reactions shown in Fig. 3 should be properly taken into account.

IV. CONCLUSIONS

We have examined all processes of the three principal pp chain branches generating MeV α particles and showed that the ^{7}Li$(p,\alpha)\alpha$ and ^{3}He$(^3$He$,2p)\alpha$ reactions play the major roles as trigger for suprathermal B(α,p)A processes in the solar CNO cycle.

The model of suprathermal processes formulated by us earlier was applied to study the effect of fast α particles on the balance of the $p + {}^{17}\mathrm{O} \rightleftarrows \alpha + {}^{14}$N reactions. It has been obtained that this balance crucially changes as compared with that for Maxwellian reactants due to a strong enhancement of the reverse (α,p) reaction caused by fast α particles. In particular, we have found that the $p + {}^7$Li α particles control

the $^{14}N(\alpha,p)^{17}O$ reaction in the inner core. At the same time, the $^{3}He + {}^{3}He$ α particles play a dominant role in the outer core and make the suprathermal effects more pronounced. It has been obtained that the $^{3}He + {}^{3}He$ α particles additionally increase the suprathermal $^{14}N(\alpha,p)^{17}O$ rate by several times (as compared with the case where these particles are ignored), providing more favorable conditions for build-up of ^{17}O.

The suprathermal reverse $^{14}N(\alpha,p)^{17}O$ reaction can block the forward $^{17}O(p,\alpha)^{14}N$ one and form a nonstandard (α,p) nuclear flow capable of altering some CNO abundances in the outer core region. Our simulations have shown that the suprathermal enhancement of the ^{17}O and ^{18}O mass fractions in the outer core can reach ~80 or 50, depending on a model for α-particle energy loss used in the calculations. In this context, we note that the $p + {}^{7}Li$ α particles alone provide the mass fraction enhancement by a factor of 20 or less [4].

ACKNOWLEDGMENTS

V. T. V. thanks L. D. Blokhintsev and C. R. Brune for useful comments on the energy spectrum of α particles produced in the low-energy $^{3}He(^{3}He,2p)\alpha$ reaction.

[1] W. A. Fowler and J. L. Vogl, *Lectures in Theoretical Physics, VI* (University of Colorado Press, Boulder, CO, 1964).
[2] V. T. Voronchev, Y. Nakao, and M. Nakamura, J. Phys. G **38**, 015201 (2011).
[3] V. T. Voronchev, Phys. Rev. C **91**, 028801 (2015).
[4] V. T. Voronchev, Y. Nakao, and Y. Watanabe, J. Phys. G **44**, 045202 (2017).
[5] E. E. Salpeter, Aust. J. Phys. **7**, 373 (1954).
[6] A. V. Gruzinov and J. N. Bahcall, Astrophys. J. **504**, 996 (1998).
[7] D. R. Tilley *et al.*, Nucl. Phys. A **745**, 155 (2004).
[8] B. Paxton, L. Bildsten, A. Dotter, F. Herwig, P. Lesaffre, and F. Timmes, Astrophys. J. Suppl. Ser. **192**, 3 (2011).
[9] Y. Xu, K. Takahashi, S. Goriely, M. Arnould, M. Ohta, and H. Utsunomiya, Nucl. Phys. A **918**, 61 (2013).
[10] E. G. Adelberger *et al.*, Rev. Mod. Phys. **83**, 195 (2011).
[11] E. G. Adelberger *et al.*, Rev. Mod. Phys. **70**, 1265 (1998).
[12] W. A. Fowler, G. R. Caughlan, and B. A. Zimmerman, Ann. Rev. Astron. Astrophys. **5**, 525 (1967).
[13] W. A. Fowler, G. R. Caughlan, and B. A. Zimmerman, Ann. Rev. Astron. Astrophys. **13**, 69 (1975).
[14] G. R. Caughlan and W. A. Fowler, At. Data Nucl. Data Tables **40**, 283 (1988).
[15] C. Iliadis, R. Longland, A. E. Champagne, A. Coc, and R. Fitzgerald, Nucl. Phys. A **841**, 31 (2010).
[16] C. Angulo *et al.*, Nucl. Phys. A **656**, 3 (1999).
[17] G. Terwagne, G. Genard, M. Yedji, and G. G. Ross, J. Appl. Phys. **104**, 084909 (2008); P. Wei, S. C. Gujrathi, M. Guihard, and F. Schiettekatte, Nucl. Instrum. Methods B **249**, 85 (2006); G. D. Mea, A. Patelli, S. Restello, V. Rigato, and A. Vomiero, *ibid.* **240**, 803 (2005); H. Xu, Z. Zhou, C. Zhang, G. Zhao, and L. Shi, *ibid.* **149**, 390 (1999); G. Giorginis, P. Misaelides, A. Crametz, and M. Conti, *ibid.* **113**, 396 (1996); H. Artigalas *et al.*, *ibid.* **66**, 237 (1992); D. F. Herring, Ren Chiba, B. R. Gasten, and H. T. Richards, Phys. Rev. **112**, 1210 (1958).
[18] D. V. Sivukhin, Rev. Plasma Phys. **4**, 93 (1966).
[19] G. Kamelander, Atomkernenergie-Kerntechnik **48**, 231 (1986).
[20] D. J. Edie, J. Vorberger, S. Rose, and D. O. Gericke, EPJ Web Conf. **59**, 05018 (2013).
[21] S. Skupsky, Phys. Rev. A **16**, 727 (1977).
[22] H. Brysk, Plasma Phys. **16**, 927 (1974).
[23] H. Brysk, P. M. Campbell, and P. Hammerling, Plasma Phys. **17**, 473 (1975).
[24] C. R. Brune, J. A. Caggiano, D. B. Sayre, A. D. Bacher, G. M. Hale, and M. W. Paris, Phys. Rev. C **92**, 014003 (2015).
[25] D. R. Tilley *et al.*, Nucl. Phys. A **708**, 3 (2004).
[26] This code was posted by F. X. Timmes at http://cococubed.asu.edu/code_pages/burn_hydrogen.shtml.
[27] M. J. Harris, D. L. Lambert, K. H. Hinkle, B. Gustafsson, and K. Eriksson, Astrophys. J. **316**, 294 (1987).
[28] M. J. Harris, D. L. Lambert, K. H. Hinkle, and V. V. Smith, Astrophys. J. **325**, 768 (1988).